The Use of Imidazolium Ionic Liquids for the Formation and Stabilization of Ir^0 and Rh^0 Nanoparticles: Efficient Catalysts for the Hydrogenation of Arenes

Gledison S. Fonseca, Alexandre P. Umpierre, Paulo F. P. Fichtner, Sergio R. Teixeira, and Jairton Dupont*[a]

Abstract: Stable transition-metal nanoparticles of the type [M^0]$_n$ are easily accessible through the reduction of Ir^I or Rh^{III} compounds dissolved in "dry" 1-n-butyl-3-methylimidazolium hexafluorophosphate ionic liquid by molecular hydrogen. The formation of these [M^0]$_n$ nanoparticles is straightforward; they are prepared in dry ionic liquid whereas the presence of the water causes the partial decomposition of ionic liquid with the formation of phosphates, HF and transition-metal fluorides. Transmission electron microscopy (TEM) observations and X-ray diffraction analysis (XRD) show the formation of [Ir^0]$_n$ and [Rh^0]$_n$ nanoparticles with 2.0–2.5 nm in diameter. The isolated [M^0]$_n$ nanoparticles can be redispersed in the ionic liquid, in acetone or used in solventless conditions for the liquid–liquid biphasic, homogeneous or heterogeneous hydrogenation of arenes under mild reaction conditions (75 °C and 4 atm). The recovered iridium nanoparticles can be reused several times without any significant loss in catalytic activity. Unprecedented total turnover numbers (TTO) of 3509 in 32 h, for arene hydrogenation by nanoparticles catalysts, have been achieved in the reduction of benzene by the [Ir^0]$_n$ in solventless conditions. Contrarily, the recovered Rh^0 nanoparticles show significant agglomeration into large particles with a loss of catalytic activity. The hydrogenation of arenes containing functional groups, such as anisole, by the [Ir^0]$_n$ nanoparticles occurs with concomitant hydrogenolysis of the C−O bond, suggesting that these nanoparticles behave as "heterogeneous catalysts" rather than "homogeneous catalysts".

Keywords: biphasic catalysis · hydrogenation · ionic liquids · iridium · nanoparticles · rhodium

Introduction

The conversion of benzene to cyclohexane is one of the most important and investigated reactions of the industrial hydrogenation processes.[1] Moreover, the increasing demand for low-aromatic petroleum-based fuels due to environmental constraints and legislation, has led to much academic and industrial research effort in order to find more simple and efficient catalytic systems.[2] In most cases this transformation is performed by employing heterogeneous catalysts[3] or in to a lesser extent with molecular catalysts under both homogeneous[1, 4] or liquid–liquid biphasic[5] conditions. However, in these cases reasonable catalytic performances were achieved under relatively drastic reaction conditions (pressure and/or temperature).

The development of new methods for the formation and stabilization of colloidal metallic particles finely dispersed in organic solvents or in water has enabled the development of one-phase or two-phase arene hydrogenation catalytic systems that operate under relatively mild reaction conditions.[6] These aqueous liquid–liquid biphasic systems are welcome improvements, in terms of product separation, catalyst recycling and catalytic performance for the hydrogenation of arenes, over the existing methods. However, transition-metal nanoparticles (usually of less than 10 nm in diameter) should be stabilized against aggregation by the use of water-soluble protective agents such as surfactants, polymers, or ionic species such as quaternary ammonium salts.[7] Moreover, it is well known, from an environmental perspective, that trace amounts of organic compounds (in particular aromatic) in water are notoriously difficult to be removed.[8] Therefore, the ideal medium for these biphasic catalytic systems will be such that it will allow not only the preparation and stabilization of transition-metal nanoparticles but will also enable easy catalyst recycling and product separation, thus avoiding the environmental problems associated with the related aqueous–organic biphasic regimes.

[a] Prof. Dr. J. Dupont, Dipl. Chem. G. S. Fonseca, Dipl. Chem. Eng. A. P. Umpierre, Prof. Dr. P. F. P. Fichtner, Prof. Dr. S. R. Teixeira
Laboratory of Molecular Catalysis—Institute of Chemistry
Department of Metallurgy Institute of Physics—UFRGS
Av. Bento Gonçalves, 9500 Porto Alegre 91501-970 RS (Brazil)
E-mail: dupont@iq.ufrgs.br

The unique physical-chemical properties of imidazolium ionic liquids,[9] such as negligible vapor pressure, relative low viscosity, high thermal, chemical and electrochemical stabilities and differentiated miscibility with organic compounds makes them ideal candidates as immobilizing agents for biphasic nanocatalysis.[10] We have recently shown that 1-*n*-butyl-3-methylimidazolium hexafluorophosphate (BMI·PF$_6$)[11] ionic liquid is a suitable medium for the preparation and stabilization of iridium nanoparticles and also ideal for the generation of recyclable biphasic catalytic systems for the hydrogenation of alkenes.[12]

We wish to report herein that this ionic liquid is also an outstanding medium for the preparation and stabilization of Rh^0 nanoparticles. Moreover, these Ir^0 and Rh^0 nanoparticles are among the most simple and efficient catalysts for the hydrogenation of arenes in solventless, "homogeneous" or liquid–liquid biphasic conditions.

Figure 2. X-ray analysis of Rh nanoparticles synthesized in "wet" (top) and "dried" (bottom) BMI·PF$_6$.

Results and Discussion

Based on our recent success in the preparation and stabilization of Ir^0 nanoparticles in BMI·PF$_6$ we applied similar reaction conditions to the preparation of Rh^0 nanoparticles. A red solution of RhCl$_3$·3H$_2$O in BMI·PF$_6$ was treated with molecular hydrogen (4 atm) at 75 °C for 1 h. The Rh^0 nanoparticles were isolated by centrifugation from the obtained black solution, washed with acetone and dried under reduced pressure. These particles were analyzed by TEM (Figure 1)
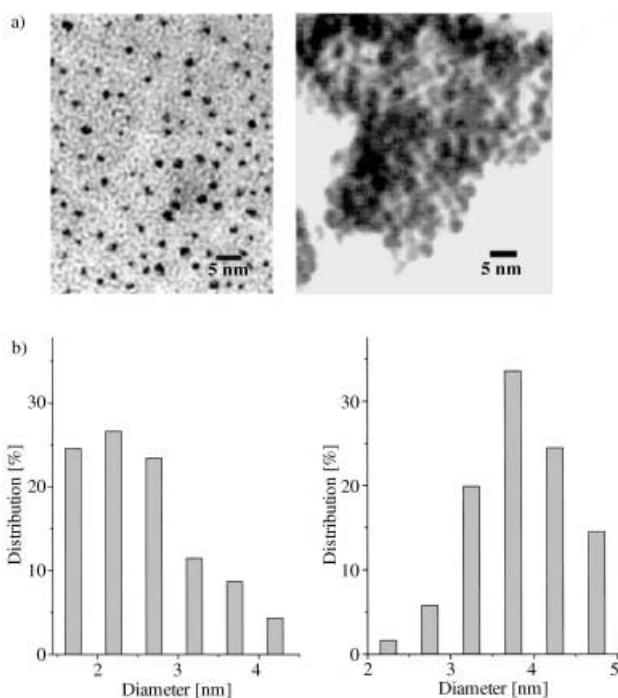

Figure 1. a) TEM micrographs showing the Rh nanoparticles observed at 200 kV (underfocus of 500 nm). Rh particles isolated before (left) and after (right) catalysis; b) histogram illustrating the particle size distribution.

and XRD (Figure 2). The particles display an irregular shape but evaluation of their characteristic diameter results in a monomodal particle size distribution that can be parameter-
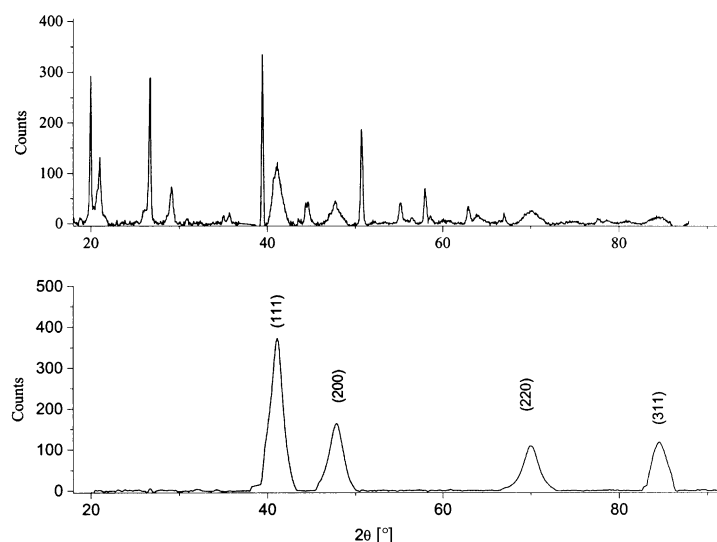
ized by a mean diameter of 2.3 nm and a standard deviation of 0.6 nm. Energy dispersion spectrometry indicates the presence of Rh and selected area diffraction shows ring patterns which can be fitted to simulation based on Rh^0 parameters. X-ray diffraction analysis also identified crystalline Rh^0 in the isolated material. The diffraction lines (111, 200, 220, 311) of metallic Rh can be clearly observed in the diffraction pattern (Figure 2). Using the Sherrer equation and assuming spherical particles, the mean diameter of the rhodium particles was estimated to be 2.5 nm from the half width of the diffraction line (111), which is in good agreement with TEM results.

Near-monodispersed Ir^0 nanoparticles with a mean diameter of 2.1 nm and a standard deviation of 0.3 nm were prepared by reduction with molecular hydrogen (4 atm) of [Ir(cod)Cl]$_2$ (cod = 1,5-cyclooctadiene) dissolved in BMI·PF$_6$ at 75 °C.[12] These particles were isolated by centrifugation and also characterized by TEM and XRD as shown in Figures 3 and 4.

It is important to note that the synthesis of Rh^0 and Ir^0 nanoparticles should be performed in the absence of water.[13] The presence of water causes the partial decomposition of the ionic liquid with the formation of phosphates (identified by ^{31}P NMR and IR), evolution of HF and rhodium or iridium fluorides isolated together with the metal nanoparticles (Figures 2 and 4). It is of note that the ionic liquid decomposition only occurs in the presence of both water and the transition-metal precursor, that is, [Ir(cod)Cl]$_2$ or RhCl$_3$, which indicates that the transition-metal is involved in the hydrolysis of the PF$_6$ anion.[14]

The isolated Ir^0 and Rh^0 nanoparticles can be used as solids ("solventless") or re-dispersed in BMI·PF$_6$ ("biphasic") or in acetone ("homogeneous") for the hydrogenation of benzene under mild reaction conditions (Table 1). In comparison with the reactions in BMI·PF$_6$, using either Ir^0 or Rh^0 nanoparticles, the reactions performed under homogeneous or "solventless" conditions require lower reaction times for their completion. This difference can be attributed to the characteristic biphasic nature of the reaction in the ionic liquid, which is
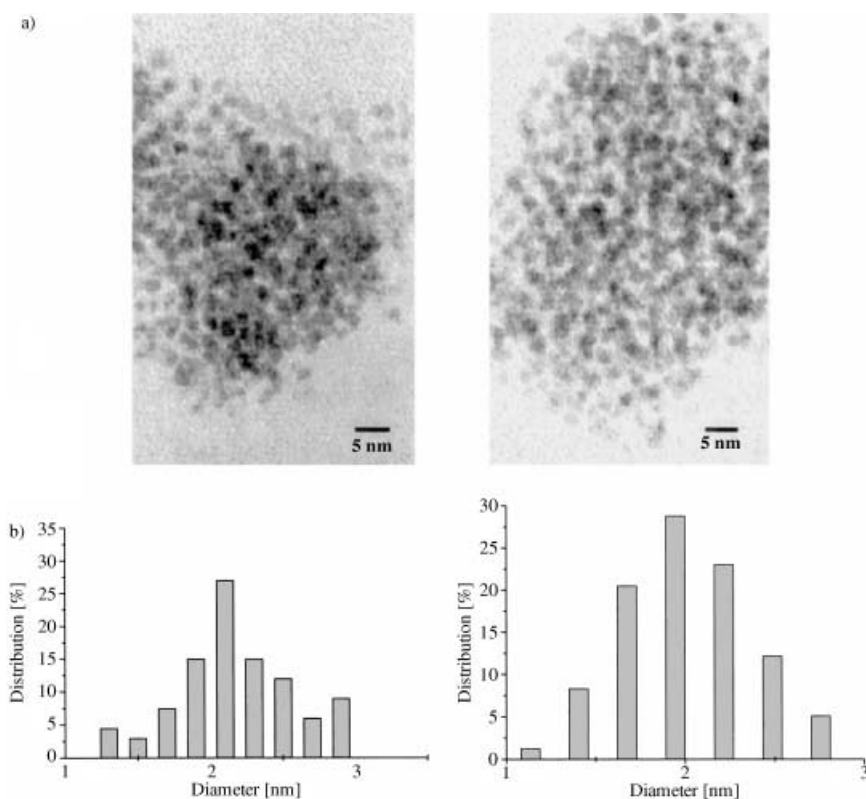
Figure 3. a) TEM micrographs showing the Ir nanoparticles observed at 200 kV (underfocus of 500 nm). Ir particles isolated before (left) and after (right) catalysis; b) histogram illustrating the particle size distribution.
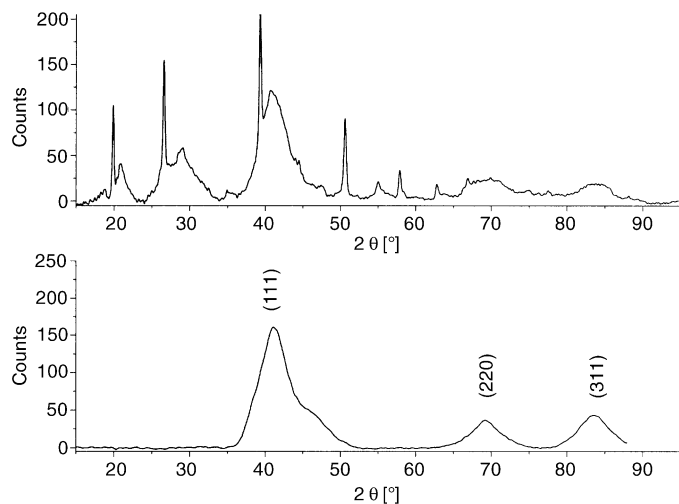

Figure 4. XRD analysis. Ir^0 nanoparticles prepared in "wet" (top) and "dried" (bottom) BMI·PF$_6$.

Notably the Ir^0 nanoparticles are isolated unchanged after catalysis (solventless), as checked by TEM and X-ray analysis. On the contrary, the Rh^0 nanoparticles isolated after catalysis show significant agglomeration into larger particles (Figure 1). Moreover, the recovered Ir^0 nanoparticles from the "solventless" run can be reused at least seven times with minimal loss in catalytic activity (Figure 5). However, those recovered from the ionic liquid show significant loss of activity due to the decomposition of both the ionic liquid and the nanoparticles (analyzed by X-ray).

A comparison of the catalytic performances of Ir^0 and Rh^0 in the hydrogenation of benzene is presented in Figure 6. It is evident that under the same reaction conditions the Ir^0 nanoparticles are much more active for the hydrogenation of ben-

Table 1. Hydrogenation of benzene with Ir^0 and Rh^0 nanoparticles at 4 atm H$_2$.[a]

	Cat.	System	[PhH]/[Metal]	t[b] [h]	TOF[c]
1	Ir	BMI·PF$_6$	250	5	50 (88)
2	Ir	BMI·PF$_6$	500	10	50 (88)
3	Ir	BMI·PF$_6$	1200	14	85 (150)
4	Ir	no solvent	500	7	71 (124)
5	Ir	no solvent	250	2	125 (219)
6	Ir	acetone	500	2.5[d]	200 (351)
7	Rh	BMI·PF$_6$	250	22	11 (21)
8	Rh	no solvent	250	12	21 (41)
9	Rh	acetone	250	16	16 (32)

[a] Reaction conditions: Constant hydrogen pressure, 75 °C, ionic liquid and acetone (1 mL). [b] Time for 100 % conversion. [c] TOF based on total metal (mol cyclohexane formed per mol metal per hour) and in parenthesis TOF corrected for exposed metal. [d] Time for complete conversion of benzene and 82 % of acetone reduction to isopropanol.

a mass-transfer controlled process.[12] The organic compounds were isolated by simple decantation or distillation under reduced pressure and analyzed by GC and GC-MS. The conversion is based on the isolated and weighed organic phase.[15] In the reactions performed under "homogeneous" conditions and Ir^0 conditions the solvent (acetone) is also hydrogenated even in the early stages of the reaction.[16] In contrast no isopropanol was detected in the reaction promoted by Rh^0 nanoparticles.

zene than their Rh^0 analogues. For example, TOF [(moles product) × (moles active site)$^{-1}$ × h^{-1}] including the corrections for the true number of active metal sites is 219 h^{-1} for [Ir^0]$_n$ and 41 h^{-1} for [Rh^0]$_n$ (entries 5 and 8, Table 1).[17]

More interestingly, both curves are sigmoidal and can be fitted to the A → B, A+B → 2 B autocatalytic mechanism that is characteristic of nanocluster formation and growth (analogous to those observed with Ir nanoparticles stabilized by polyoxoanions). This suggests that this autocatalytic process could be a more general case in transition-metal nanoparticle formation, as proposed earlier by Finke.[18]
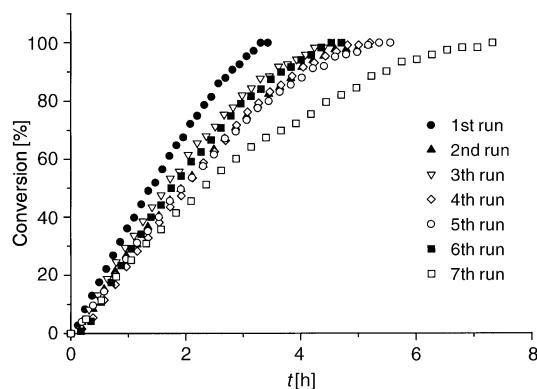
Figure 5. Conversion curves of benzene hydrogenation by Ir^0 nanoparticles "solventless" at 4 atm and 75 °C, [benzene]/[Ir] = 250, showing the catalyst recycle.
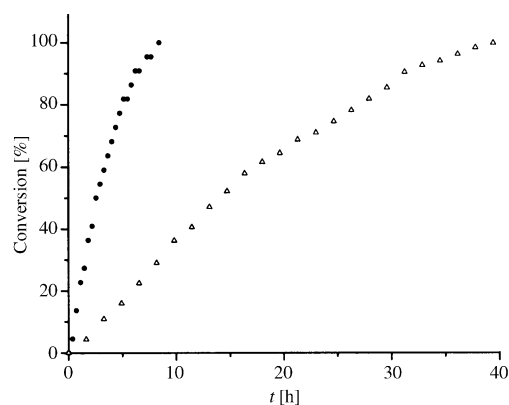

Figure 6. Curve of conversion of benzene hydrogenation catalyzed by (left) Ir^0 and (right) Rh^0 nanoparticles prepared in situ in $BMI \cdot PF_6$ (1 mL) at 75 °C and 4 atm (constant pressure). [M]/[substrate] ratio 1:500 (1200 rpm).

These nanoparticles, either dispersed in the $BMI \cdot PF_6$ or as a "solventless" system, are also efficient catalysts for the hydrogenation of other aromatic compounds (Table 2).

At this stage of our studies we do not have direct evidence of the mechanism involved in these hydrogenation reactions although the relatively low selectivity in *cis*-1,4-dimethylcyclohexane (entries 2, 3 and 8, Table 2) indicates that in these nanocatalytic processes the slippage mechanism is not predominant.[19] Indeed, small quantities of cyclohexene (12% in selectivity) could be detected in the earlier stages of hydrogenation of benzene (conversions <1%) by $[Rh^0]_n$ nanoparticles in both biphasic and solventless conditions.

Although the hydrogenolysis of arenes is almost a general case in the hydrogenation of arenes by soluble transition-metal nanoparticles,[7] it is much slower compared with the aromatic ring reduction. However, with only one exception involving the hydrogenation of dibenzo-[18]crown-6 ether,[20] the hydrogenolysis products are generally only detected in small quantities.[21] We have observed that the hydrogenolysis products, ethylcyclohexane and cyclohexane, are formed in relatively high quantities (up to 42%) in the "solventless" hydrogenation of acetophenone and anisole, respectively, by $[Ir^0]_n$ (Scheme 1 and entries 5 and 6, Table 2). Interestingly, in the reactions catalyzed by $[Rh^0]_n$ no hydrogenolysis products were observed in the hydrogenation of anisole.
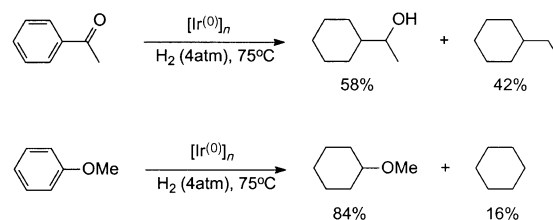
Scheme 1.

Most importantly, the fact that hydrogenolysis of the C−O bond occurs which is characteristic of a surface metal catalyst,[1] suggests that these nanoparticles behave preferentially as "heterogeneous catalysts" rather than a "homogeneous catalysts", in terms of active sites.[22]

Although it remains to be proven exactly how the $BMI \cdot PF_6$ ionic liquid is acting in the formation and stabilization of the nanoparticles,[23] it is reasonable to assume that the combined

Table 2. Hydrogenation of arenes by Ir^0 (0.026 mmol) and Rh^0 (0.1 mmol) nanoparticles dispersed in $BMI \cdot PF_6$ (1 mL) and solventless system at 75 °C and 4 atm.[a]

	M	System	Arene	Products	[ArH]/[M]	t [h]	Conv[b] [%]	TOF[c]
1	Ir	$BMI \cdot PF_6$	toluene	methylcyclohexane	1200	25	93	44 (78)
2	Ir	$BMI \cdot PF_6$	*p*-xylene	*p*-dimethylcyclohexane	500	18	86[d]	24 (42)
3	Ir	solventless	*p*-xylene	*p*-dimethylcyclohexane	250	12	100[e]	21 (36)
4	Ir	solventless	methylbenzoate	cyclohexylmethylcarboxylate	250	18	92	13 (22)
5	Ir	solventless	acetophenone	ethylcyclohexane and 1-cyclohexylethan-1-ol	250	16	100[f]	15 (27)
6	Ir	solventless	anisole	methoxycyclohexane and cyclohexane	250	18	74[g]	10 (18)
7	Rh	solventless	toluene	methylcyclohexane	250	22	62	7 (14)
8	Rh	$BMI \cdot PF_6$	*p*-xylene[h]	*p*-dimethylcyclohexane	250	12	26[i]	5 (10)
9	Rh	solventless	methylbenzoate	cyclohexylmethylcarboxylate	250	14	58	10 (20)
10	Rh	$BMI \cdot PF_6$	anisole	methoxycyclohexane	250	6	100	41 (82)

[a] Constant positive pressure. [b] Conversion. [c] TOF based on total metal (mol cyclohexane formed per mol metal per h) and in parenthesis TOF corrected for exposed metal. [d] *cis/trans* 5: 1. [e] *cis/trans* 3: 1. [f] 42% ethylcyclohexane and 58% 1-cyclohexyl-1-ethanol. [g] 84% of methoxycyclohexane and 16% of cyclohexane. [h] 50 atm. [i] *cis/trans* 2: 1.

 www.chemeurj.org *Chem. Eur. J.* **2003**, *9*, 3263–3269

intrinsic high charge plus the steric bulk of these salts, which can be described as polymeric supramolecules with weak interactions,[24] can create an electrostatic and steric colloid-type stabilization of transition-metal nanoparticles, similar to the model suggested by Finke[7] in the stabilization of nanoclusters by polyoxoanions or by tetralkylammonium salts employed by Reetz[25] but as explained correctly by others.[18]

Conclusion

In summary we have shown that $BMI \cdot PF_6$ is an outstanding medium for the preparation and stabilization of Rh^0 and Ir^0 nanoparticles of 2 – 3 nm diameter and narrow size distribution. These $[Ir^0]_n$ nanoparticles are outstanding catalysts for the hydrogenation of arenes and they do behave as heterogeneous catalysts.

Experimental Section

General methods: All reactions involving iridium and rhodium compounds were carried out under argon atmosphere in oven dried Schlenk tubes. The $BMI \cdot PF_6$ ionic liquid was prepared according to known procedure[9] dried over molecular sieves (4 Å) and its purity was checked by $AgNO_3$ test, ^1H and ^{31}P NMR spectra, and cyclic voltametry. The water[13] (< 0.1 wt %) and chloride[26] (< 1.4 mg L^{-1}) contents in $BMI \cdot PF_6$ used were determined by known methods. Solvents and arenes were dried with adequate drying agents and distilled under argon prior to use. All the other chemicals were purchased from commercial sources and used without further purification. NMR spectra were recorded on a Varian Inova 300 spectrometer. Infrared spectra were performed on a Bomem B-102 spectrometer. Mass spectra were obtained using a GC/MS Shimadzu QP-5050 (EI, 70 eV). Gas chromatography analyses were performed with a Hewlett – Packard 5890 gas chromatograph with a FID and 30 m capillary column with a dimethylpolysiloxane stationary phase. The X-ray diffraction was performed in a Philips X Pert MRD diffractometer in a Bragg – Brentano geometry using curved graphite crystal as monocromator. Transmission electron microscopy (TEM) was performed on a JEOL 2010 microscope operating at 200 kV. The TEM images were obtained in bright-field conditions using a 20 μm objective aperture and with the objective bus slightly underfocused ($\Delta f \sim -500$ nm).

Reaction conditions: The nanoparticles formation and hydrogenation reactions were carried out in a modified Fischer – Porter bottle immersed in a silicon oil bath and connected to a hydrogen tank. The decrease in the hydrogen pressure in the tank was monitored with a pressure transducer interfaced through a Novus converter to a PC and the data workup via Microcal Origin 5.0. The temperature was maintained at 75 °C by a hot stirring plate connected to a digital controller (ETS-D4 IKA). A deliberated stirring at 1200 rpm was used (no ionic catalytic solution projection was observed). The catalyst/substrate ratio was calculated from the initial quantity of $[Ir(cod)Cl]_2$ or $RhCl_3 \cdot 3H_2O$ used.

Nanoparticles formation and isolation: In a typical experiment a Fischer – Porter bottle containing an yellow solution of $[Ir(cod)Cl]_2$ (16 mg, 0.05 mmol) in dichloromethane (3 mL) or $RhCl_3 \cdot 3H_2O$ (26 mg, 0.1 mmol) was added to $BMI \cdot PF_6$ (1 mL) and stirred at room temperature for 15 min. The volatiles were then removed under reduced pressure (0.1 bar) at 75 °C for 1 h. The system was kepted at 75 °C and hydrogen (4 bar) was admitted to the system. After stirring for 10 min (Ir) or 1 h (Rh) a black "solution" was obtained that was used for the hydrogenation reactions or isolation of the nanoparticles. The Ir nanoparticles were isolated by centrifugation (3000 rpm) for 5 min and washed with acetone (3 × 15 mL) and dichloromethane (3 × 15 mL) and dried under reduced pressure. The Ir and Rh samples thus obtained were prepared for TEM and X-ray analysis, and for catalytic experiments (see below).

Hydrogenations

Liquid – liquid biphasic: The arene was added to the ionic catalytic solution obtained was described above and hydrogen was admitted to system at constant pressure (see Tables 1 and 2). Samples for GC and GC-MS analysis were also removed from time to time under H_2. The reaction mixture forms a typical two-phase system (lower phase containing the Ir or Rh nanoparticles in the ionic liquid and upper phase the organic products). The organic phase was separated by decantation or distillation, weighted and analyzed by GC. GC-MS and ^1H NMR.

Solventless: The isolated nanoparticles were placed in a Fischer – Porter bottle and the arene was added. The reactor was placed in a oil bath at 75 °C and hydrogen was admitted to the system at constant pressure (4 atm). Samples for GC and GC-MS analysis were also removed from time to time under H_2. The organic products were recovered by simple filtration and analyzed by GC.

Homogeneous: The isolated nanoparticles were dispersed in acetone (3 mL) placed in a Fischer – Porter bottle and the arene was added. The reactor was placed in an oil bath at 75 °C and hydrogen was admitted to the system at constant pressure (4 atm). Samples for GC and GC-MS analysis were also removed from time to time under H_2. The organic products were recovered by simple filtration and analyzed by GC.

Identification of cyclohexene in the hydrogenation of benzene: The identification of cyclohexene was unequivocally established by GC-MS and by GC retention time versus authentic sample of cyclohexene (Acros). GC was performed using a 100 m capillary column with a dimethylpolysiloxane stationary phase. (0.25 mm × 0.5 μm). The GC parameters were: initial temperature 50 °C; initial time 10 min; temperature ramp 10 °C min^{-1}; final temperature 250 °C; detector and injector port temperature 250 °C and injection volume 0.1 μL.

Sample preparation and TEM analysis: The samples were prepared according to the following methods: a) acetone suspension of the Ir or Rh nanoparticles was deposited on a formvar covered carbon coated grid (300 mesh). b The nanoparticles were mixed with a epoxy resin distributed between two silicon wafer pieces at 50 °C for 30 min. Cross-section TEM samples were pre-thinned mechanically. The thinning to electron transparency was obtained by ion milling. Particle size distributions were determined once the original negative had been digitalized and expanded to 470 pixels per cm for more accurate resolution and measurement. Typically, TEM pictures of each sample at multiple random locations in the sample and at two different magnifications. The size distribution histogram was obtained on the basis of measurement of about 300 particles. The EDS and electronic diffraction analysis of the $[Ir^0]_n$ and $[Rh^0]_n$ are presented in Figures 7 – 10.

Sample preparation and X-ray analysis: The Ir powder was mixed with vacuum grease and fixed on a glass substrate. A flat surface was obtained pressing the mixed powder between two flat glasses. The diffraction pattern was obtained after subtraction of the powder spectrum from a background measured using a glass substrate plus the vacuum grease.

The final spectrum is composed by very broad peaks corresponding to nanoparticles of metallic Ir. Assuming spherical particles their mean size can be obtained from the well known Sherrer Equation
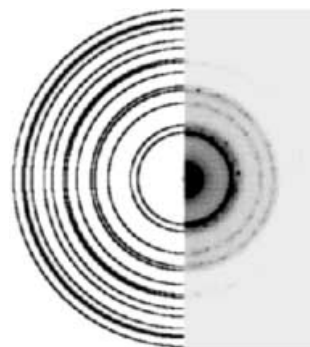

Figure 7. Electron Diffraction Micrograph obtained by TEM of the Ir particles after the catalytic reaction. Iridium ring pattern theoretical (left) and experimental (right).
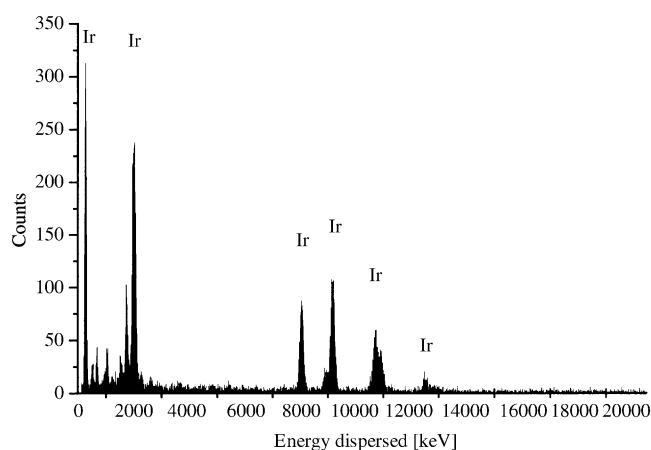
Figure 8. EDS of the Ir^0 nanoparticles prepared in $BMI \cdot PF_6$, 75 °C, H_2 (4 atm), 10 min.
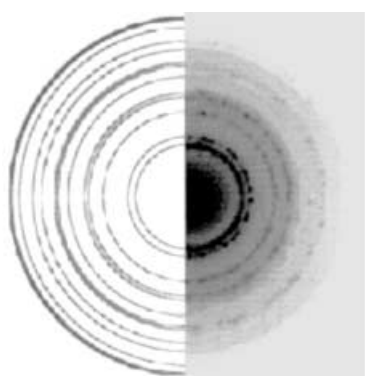

Figure 9. Electron diffraction micrograph obtained by TEM of the Rh particles. Rhodium ring pattern theoretical (left) and experimental (right).
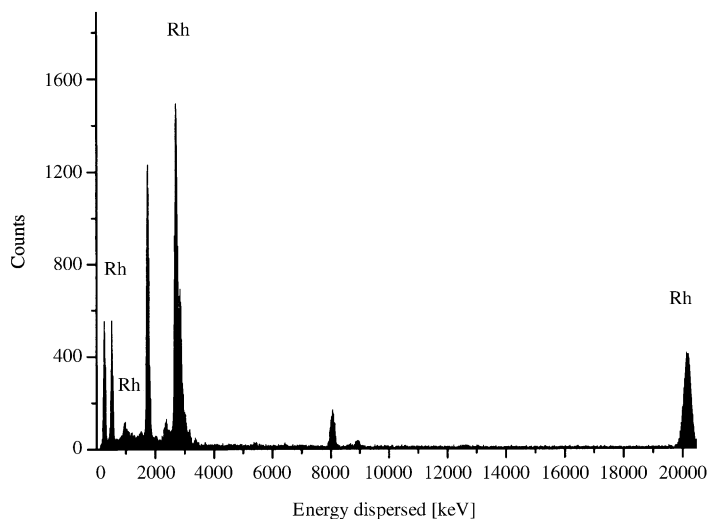

Figure 10. EDS of the Rh^0 nanoparticles prepared in $BMI \cdot PF_6$, 75 °C, H_2 (4 atm), 1 h.

$$L = \frac{K\lambda}{\beta_{1/2} \cos\theta} \tag{1}$$

where L is the mean diameter of the nanoparticles, $\beta_{1/2}$ is the full width at half maximum of the diffraction peak, θ is the Bragg angle for a given set $\{hkl\}$ planes, λ is the wave length of the $Cu_{K\alpha}$ radiation (1.5406 Å) and $K = 0.893$ for spheres. For more information see ref. [27].

[1] a) G. W. Parshall, S. D. Ittel, *Homogeneous Catalysis*, Wiley-Interscience, New York, **1992**; b) *An Integrated Approach to Homogeneous, Heterogeneous and Industrial Catalysis* (Eds.: J. A. Moulijn, P. W. N. M. van Leeuwen, R. A. van Santen), Elsevier, Amsterdam, **1995**; c) *Applied Homogeneous Catalysis with Organometallic Compounds* (Eds.: B. Cornils, W. A. Herrmann), VCH, Weinheim, **1996**.

[2] a) A. Stanislaus, B. H. Cooper, *Catal. Rev.* **1994**, *36*, 75; b) M. L. Occelli, R. Chianelli, *Hydrotreating Technology for Polution Control*, Marcel Dekker, New York, **1996**.

[3] See for example: a) J. Scherzer, A. J. Guia, *Hydrocracking Science and Technology*, Marcel Dekker, New York, **1996**; b) H. Gao, R. Angelici, *J. Am. Chem. Soc.* **1997**, *119*, 6937; c) J. Goulon, E. Georges, C. Goulonginet, Y. Chauvin, D. Commereuc, H. Dexpert, E. Freund, *Chem. Phys.* **1984**, *83*, 357.

[4] See for example: I. P. Rothwell, *Chem. Commun.* **1997**, 1331.

[5] a) G. Suss-Fink, M. Faure, T. R. Ward, *Angew. Chem.* **2002**, *114*, 105; *Angew. Chem. Int. Ed.* **2002**, *41*, 99; b) P. J. Dyson, D. J. Ellis, D. G. Parker, T. Welton, *Chem. Commun.* **1999**, 25; c) C. J. Boxwell, P. J. Dyson, D. J. Ellis, T. Welton, *J. Am. Chem. Soc.* **2002**, *124*, 9334.

[6] a) J. L. Pellegatta, C. Blandy, V. Colliere, R. Choukroun, B. Chaudret, P. Cheng, K. Philippot, *J. Mol. Catal. A Chem.* **2002**, *178*, 55; b) J. Schulz, A. Roucoux, H. Patin, *Chem. Eur. J.* **2000**, *6*, 618; c) J. Schulz, A. Roucoux, H. Patin, *Chem. Commun.* **1999**, 535; d) K. S. Weddle, J. D. Aiken, R. G. Finke, *J. Am. Chem. Soc.* **1998**, *120*, 5653; e) J. A. Widegreen, R. G. Finke, *J. Mol. Catal. A Chem.* **2003**, *191*, 187.

[7] For recent reviews see: a) R. G. Finke in *Transition-Metal Nanoclusters* (Eds.: D. L. Feldheim, C. A. Foss, Jr.), Marcel Dekker, New York, **2002**, Chapter 2, pp. 17–54; b) J. D. Aiken, R. G. Finke, *J. Mol. Catal. A Chem.* **1999**, *145*, 1; c) H. Bonnemann, R. M. Richards, *Eur. J. Inorg. Chem.* **2001**, 2455.

[8] R. W. Cusack, *Chem. Eng. Prog.* **1996**, *92*, 56.

[9] a) P. A. Z. Suarez, S. Einloft, J. E. L. Dullius, R. F. de Souza, J. Dupont, *J. Chim. Phys. Chim. Biol.* **1998**, *95*, 1626; b) J. E. L. Dullius, P. A. Z. Suarez, S. Einloft, R. F. de Souza, J. Dupont, J. Fischer, A. De Cian, *Organometallics* **1998**, *17*, 815.

[10] For recent reviews see: a) T. Welton, *Chem. Rev.* **1999**, *99*, 2071; b) P. Wasserscheid, W. Keim, *Angew. Chem.* **2000**, *112*, 3926; *Angew. Chem. Int. Ed.* **2000**, *39*, 3772; c) R. Sheldon, *Chem. Commun.* **2001**, 2399; d) J. Dupont, R. F. de Souza, P. A. Z. Suarez, *Chem. Rev.* **2002**, *102*, 3667.

[11] a) P. A. Z. Suarez, J. E. L. Dullius, S. Einloft, R. F. deSouza, J. Dupont, *Polyhedron* **1996**, *15*, 1217; b) J. Dupont, C. S. Consorti, P. A. Z. Suarez, R. F. deSouza, *Org. Synth.* **2002**, *79*, 236.

[12] J. Dupont, G. S. Fonseca, A. P. Umpierre, P. F. P. Fichtner, S. R. Texeira, *J. Am. Chem. Soc.* **2002**, *124*, 4228.

[13] Cyclic Voltametry can detect the presence of traces amounts of water: B. K. Sweeny, D. G. Peters, *Electrochem. Commun.* **2001**, *3*, 712. The ionic liquid was dried over molecular sieves (4 Å) before use.

[14] For studies on the hydrolysis of the hexafluorophosphate anion see: a) P. Pelletier, J. Durand, L. Cot, *Z. Anorg. All. Chem.* **1990**, *581*, 190; b) H. R. Clark, R. Clark, M. M. Jones, *Inorg. Chem.* **1971**, *10*, 28; for the decomposition of $BMI \cdot PF_6$ see: J. Dupont, S. M. Silva, R. F. de Souza, *Catal. Lett.* **2001**, *77*, 131.

[15] Benzene has a miscibility of 0.66 solute mole fraction with $BMI \cdot PF_6$ and cyclohexane has a value of 0.21. L. A. Blanchard, J. F. Brennecke, *Ind. Eng. Chem. Res.* **2001**, *40*, 287.

[16] The use of the Ir^0 nanoparticles for the hydrogenation of C=O bonds is currently under investigation.

[17] The TOF corrected for exposed metal was obtained using a known method as reported earlier by Finke: B. J. Hornstein, J. D. Aiken III, R. G. Finke, *Inorg. Chem.* **2002**, *41*, 1625.

[18] a) M. A. Watzky, R. G. Finke, *Chem. Mater.* **1997**, *9*, 3083; b) S. Ozkar, R. G. Finke, *J. Am. Chem. Soc.* **2002**, *124*, 5796.

[19] R. L. Augustine, *Heterogeneous Catalysis for the Synthetic Chemistry*, Marcel Dekker, New York, **1996**, Chapter 17.

[20] P. D. Landre, D. Richard, M. Draye, P. Gazellot, M. Lemaire, *J. Catal.* **1994**, *147*, 214.

[21] J. A. Widegren, R. G. Finke, *Inorg. Chem.* **2002**, *41*, 1558.

[22] a) J. Schwartz, *Acc. Chem. Res.* **1985**, *18*, 302; b) J. D. Aiken, Y. Lin, R. G. Finke, *J. Mol. Catal. A Chem.* **1996**, *114*, 29.

[23] At this stage of our studies we cannot entirely discard that chloride anions (present in the transition-metal precursors or residual in the ionic liquid) could be responsible for the stabilization of nanoparticles, as pointed out by one of the referees. However, EDS analysis of the nanoparticles re-dispersed in the ionic liquid, as well as in their surroundings indicates only the presence of Ir, P and F atoms. Within the detection limit of the EDS technique the presence of chloride could not be detected. Moreover, we have found that the presence of residual chloride anions in the ionic liquid suppresses the formation of the nanoparticles as well as the catalytic activity of the re-dispersed nanoparticles in BMI·PF₆.

[24] a) U. Schroder, J. D. Wadhawan, R. G. Compton, F. Marken, P. A. Z. Suarez, C. S. Consorti, R. F. de Souza, J. Dupont, *New J. Chem.* **2000**, *24*, 1009; b) J. Dupont, P. A. Z. Suarez, R. F. de Souza, R. A. Burrow, J. P. Kintzinger, *Chem. Eur. J.* **2000**, *6*, 2377.

[25] M. T. Reetz, W. Helbig, S. A. Quaiser, U. Stimming, N. Breuer, R. Vogel, *Science* **1995**, *267*, 367.

[26] V. Gallo, P. Mastrorilli, C. F. Nobile, G. Romanazzi, G. P. Suranna, *J. Chem. Soc. Dalton Trans.* **2002**, 4339.

[27] J. W. Niemantsverdriet, *Spectroscopy in Catalysis*, VCH, Weinheim, **1995**.